




Cite this: *Chem. Sci.*, 2024, 15, 9582

All publication charges for this article have been paid for by the Royal Society of Chemistry

Acridine photocatalysis enables tricomponent direct decarboxylative amine construction†

Xianwei Sui,  Hang T. Dang,  Arka Porey, Ramon Trevino, Arko Das, Seth O. Fremin, William B. Hughes, William T. Thompson, Shree Krishna Dhakal, Hadi D. Arman and Oleg V. Larionov *

Amines are centrally important motifs in medicinal chemistry and biochemistry, and indispensable intermediates and linchpins in organic synthesis. Despite their cross-disciplinary prominence, synthetic access to amine continues to rely on two-electron approaches based on reductions and additions of organometallic reagents, limiting their accessible chemical space and necessitating stepwise preassembly of synthetic precursors. We report herein a homogeneous photocatalytic tricomponent decarboxylative radical-mediated amine construction that enables modular access to α -branched secondary amines directly from the broad and structurally diverse chemical space of carboxylic acids in a tricomponent reaction with aldehydes and aromatic amines. Our studies reveal the key role of acridine photocatalysis acting in concert with copper and Brønsted acid catalytic processes in facilitating the previously inaccessible homogeneous photocatalytic reaction and provide a streamlined segue to a wide range of amines and nonproteinogenic α -amino acids.

Received 9th April 2024

Accepted 20th May 2024

DOI: 10.1039/d4sc02356k

rsc.li/chemical-science

Introduction

Homogeneous photocatalytic systems have recently received significant attention due to their ability to catalyze a broad range of complex synthetic transformations.¹ Advantageously, homogeneous photocatalysts can effect light-driven reactions at low catalyst loadings and are readily accessible. Furthermore because of their modularity, they can be easily modified, enabling facile reaction optimization. However, homogeneous photocatalytic systems that are based on non-directional single electron transfer are prone to overoxidizing low oxidation potential reactants and products, catalyst deactivation, as well as other radical-based side processes resulting from the high diffusion rates observed in solution phase reactions.¹ Consequently, the development of chemoselective homogeneous photocatalytic reactions, especially those that involve complex multicomponent and multicatalytic manifolds, remains a significant challenge (Fig. 1).

Continued progress in chemical, biomedical, and materials sciences relies on the development of new synthetic transformations that can provide rapid access to new chemical space and molecular complexity.² α -Branched amines are ubiquitous structural motifs in therapeutic and agricultural agents, natural products, synthetic intermediates, catalysts, and advanced

Department of Chemistry, The University of Texas at San Antonio, One UTSA Circle, San Antonio, TX 78249, USA. E-mail: oleg.larionov@utsa.edu

† Electronic supplementary information (ESI) available. CCDC 2340500, 2340502, 2340501, 2340499, 2340503. For ESI and crystallographic data in CIF or other electronic format see DOI: <https://doi.org/10.1039/d4sc02356k>

A. Amines and approaches to their construction



B. Direct decarboxylative tricomponent construction of α -branched amines enabled by acridine photocatalysis

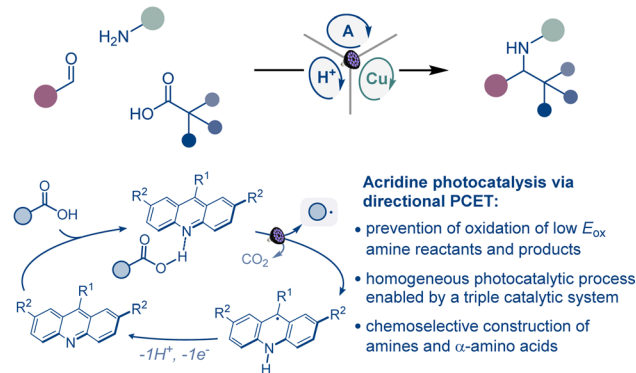


Fig. 1 Direct decarboxylative construction of α -branched amines.



materials, where the conformational features and the proximity of the amino group to other functionalities in the branched chain define the properties and function of the molecule. For example, the π system in α -aromatic amines provides a combination of conformational rigidity and multivector noncovalent interactions with the aromatic ring and the basic nitrogen atom, facilitating molecular recognition and binding that are key to their applications in medicinal chemistry and catalysis.³ Likewise, nonproteinogenic α -amino acids are widely used to improve stability, potency, permeability, and oral bioavailability of peptide therapeutics,⁴ while sterically encumbered amino acids bearing tertiary alkyl groups in the side chain are key structural elements of catalysts and ligands.⁵

Despite their cross-disciplinary importance, synthetic access to α -branched amines continues to rely on reductive amination or additions of organometallic reagents that necessitate pre-assembly of the ketone and imine precursors or may be incompatible with base-sensitive functionalities.⁶ By contrast, modular approaches that enable the formation of the imine intermediate and the ensuing formation of the C–N bond in the same reaction can significantly streamline access to α -branched amines. Critically, the success of this approach hinges on the mutual compatibility of both processes, posing a challenge to the reaction design. However, recent examples of radical-mediated modular tricomponent α -branched amine construction by combining aldehydes and amines with alkyl halides, alkyldihydropyridines, and trifluoroborates point to the feasibility of the approach.⁷

Carboxylic acids are among some of the most abundant and structurally diverse feedstocks that are produced by the chemical industry, as well as derived from natural products, and commonly used as synthetic intermediates. A direct tricomponent decarboxylative reaction of carboxylic acids with aldehydes and amines effected by a homogeneous photocatalytic system could provide a modular synthetic shortcut that will expand the accessible chemical space of α -branched amines, leveraging the broad span of the chemical space of carboxylic acids across the domains of molecular complexity,⁸ fraction of sp^3 carbon atoms (F_{sp^3}),⁹ and geometric diversity.^{10,11}

A broad-scope homogeneous photocatalytic reaction of this type would obviate the stepwise preassembly of imine precursors and the use of *N*-sulfonylimine substrates, as well pre-activation of carboxylic acids that is typically required to circumvent the challenging oxidative cleavage of the carboxylic group, whose high oxidation potential renders the process incompatible with amines and other easily oxidizable functionalities under homogeneous photocatalytic conditions.¹² Given the complexity of the process and the potential for over-oxidation of easily oxidizable substrates, a homogeneous photocatalytic system that can enable the transformation has remained elusive, and only single example with a heterogeneous superstoichiometric inorganic semiconductor has been described.¹³ As a result, the scope of the direct decarboxylative tricomponent amine construction remains limited and does not permit construction of synthetically important nitrogenous compounds, for example nonproteinogenic α -amino acids.¹⁴ Additionally, the development of a homogeneous photocatalytic

system that efficiently mediates direct decarboxylative tricomponent amine construction will provide insight into mechanisms of multicomponent photocatalytic processes and facilitate the design of other currently unavailable chemo-selective multicomponent transformations.

Acridine photocatalysis has recently emerged as a new catalytic platform for direct decarboxylative functionalization that has demonstrated broad scope and compatibility with a variety of easily oxidizable functionalities.^{15–17} The chemo-selectivity of the acridine-catalyzed direct decarboxylation is due to the directional character of the decarboxylative process within the acridine–carboxylic acid complex that undergoes photoinduced proton-coupled electron transfer (PCET). Despite the progress, the scope of the functionalizations that can be facilitated by acridine photocatalysis remains ill-defined.

We report herein the development of acridine-catalyzed decarboxylative tricomponent construction of α -branched amines directly from carboxylic acids, aldehydes, and aromatic amines that provides a pipeline to the broad chemical space of carboxylic acids.¹⁸ The modular synthesis is enabled by a choreographed interplay of the acridine photocatalysis with copper and Brønsted acid catalytic cycles. The reaction provides direct access to a wide range of α -branched amines including an array of nonproteinogenic α -amino acid derivatives. Mechanistic studies point to key roles of each of the three intertwined catalytic cycles in enabling the modular construction of α -branched amines that obviates preassembly and preactivation of amines and carboxylic acids.

Results and discussion

After initial optimization studies, we found that a reaction of aldehyde **1**, aniline **2**, and carboxylic acid **3** efficiently produced amine **4a** with acridine catalyst **A1**, as well as copper(i) and sulfonic acid co-catalysts under 400 nm LED irradiation (Fig. 2). Structurally related acridines **A2** and **A3** were also competent,



Fig. 2 Reaction conditions for the photocatalytic direct decarboxylative tricomponent amine construction: aldehyde **1** (0.2 mmol), aniline **2** (0.24 mmol), carboxylic acid **3** (0.2 mmol), acridine **A1** (8 mol%), Cu(MeCN)₄BF₄ (8 mol%), TsOH (8 mol%), MeCN (2 mL), 4 Å molecular sieves (60 mg), LED light (400 nm), 30 h. Yield was determined by ¹H NMR spectroscopy with 1,3,5-trimethoxybenzene as an internal standard. ^aIsolated yield.



albeit slightly less effective catalysts (Fig. 2A), and the reaction required light and the acridine catalyst to proceed (Fig. 2B). The copper(I) catalyst was also essential for the reaction, and a significantly lower yield was observed in the absence of the sulfonic acid. A lower yield was also observed without molecular sieves. Likewise, the reaction was less efficient in other solvents and with other copper co-catalysts (Fig. 2B). Significantly, no amine formation was observed with other types of photocatalysts, *e.g.*, Ir- and Ru-based photocatalysts, 4CzIPN, *N*-phenyl 9-mesitylacridinium salts, and eosin Y (Table S1†).

The scope of aromatic amines was examined next in a reaction with aldehyde **2** and carboxylic acid **3** (Scheme 1). Anilines bearing alkyl groups were readily converted to the corresponding amines **4b–4d**. A full range of halogen (**4e–4h**), methoxy (**4i**), thiomethoxy (**4j**), and trifluoromethoxy-substituted (**4k**) anilines were also suitable coupling partners. *N*-substituted biphenyl amines **4l** and **4m** were accessed in good yields. Amines **4n–4p** bearing a boron group in the *meta*, *para*, and *ortho* positions were likewise smoothly constructed. Anilines bearing heteroaryl groups also afforded corresponding amines **4q–4r**, however, *o*-, *m*-, and *p*-aminopyridines were not compatible with the reaction.

A range of aromatic aldehydes were examined next (Scheme 2). Aldehydes bearing alkyl (**5a–5c**), halogen (**5d**, **5e**), and methoxy (**5f**, **5g**) groups in the *meta*, *para*, and *ortho* positions were well tolerated. Amines featuring amide (**5h**), and trifluoromethyl (**5i**) groups in the benzylic aryl ring were

similarly readily synthesized. Both isomeric naphthaldehyde precursors produced the corresponding amines **5j** and **5k** in excellent yields. Heteroaromatic aldehydes were also suitable coupling partners, and a range of amines containing pyridine (**5l** and **5m**), benzofuran (**5n**), and indole (**5o**, **5p**) were efficiently produced in a single step.

We next explored the scope of carboxylic acids (Scheme 3). An array of primary and secondary acyclic and cyclic carboxylic acids were converted to amines **6a–6h**, including amines featuring small-ring and saturated heterocyclic systems (**6e**, **6h**). Likewise, a variety of tertiary carboxylic acids were also suitable reactants, affording amines **6i–6n** that bear acyclic, cyclic, and caged topologies in the alkyl moiety.

Given the cross-disciplinary importance of nonproteinogenic α -amino acids, we examined the tricomponent decarboxylative reaction with glyoxylates as aldehyde components (Scheme 4). *p*-Methoxyaniline ($E_{1/2} = -0.24$ V vs. SCE¹⁹) was selected as an amine to test if easily oxidizable anilines are tolerated in the photocatalytic reaction and because of the well-documented protocols for the removal of the PMP group in the context of α -amino acid synthesis.²⁰ Norleucine (**7a**) and homoleucine (**7b**), as well as long-chain (**7c**) and trifluoromethyl-substituted (**7d**) amino acid derivatives were readily accessed from the corresponding carboxylic acids. Amino acid derivatives **7e–7i** bearing aromatic substituents, including sterically encumbered (**7e**) and halogen containing (**7f**, **7g**) analogues of phenylalanine and homophenylalanine were similarly easily prepared in

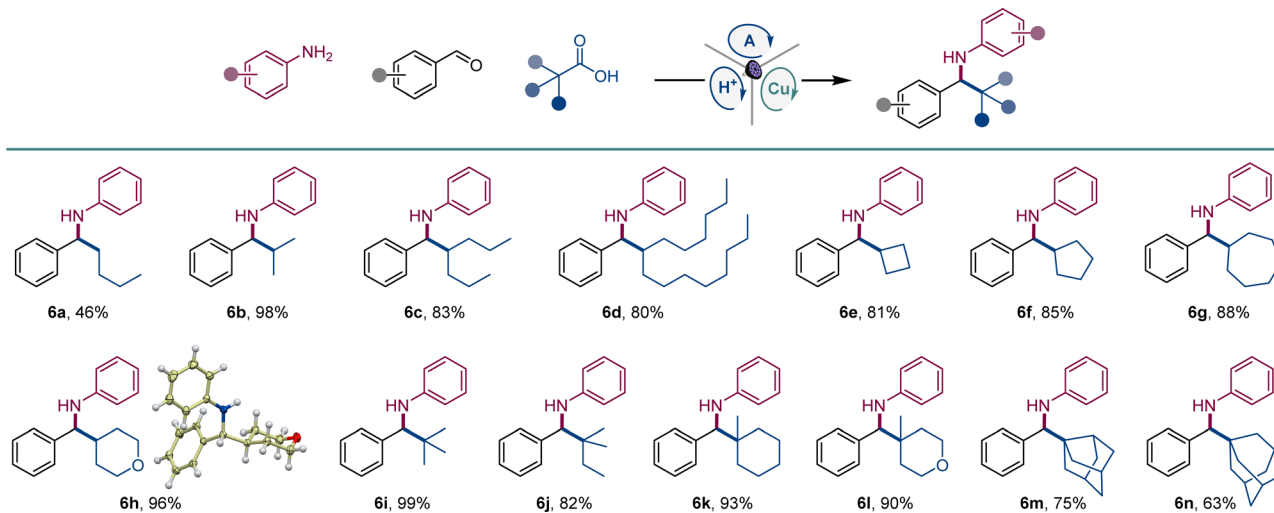


Scheme 1 Scope of anilines in the direct decarboxylative tricomponent amine construction. Reaction conditions: aldehyde **1** (0.2 mmol), aniline **2** (0.24 mmol), carboxylic acid **3** (0.2 mmol), acridine **A1** (8 mol%), Cu(MeCN)₄BF₄ (8 mol%), TsOH (8 mol%), MeCN (2 mL), 4 Å molecular sieves (60 mg), LED light (400 nm), 30 h.





Scheme 2 Scope of aldehydes in the direct decarboxylative tricomponent amine construction. Reaction conditions: see Scheme 1.

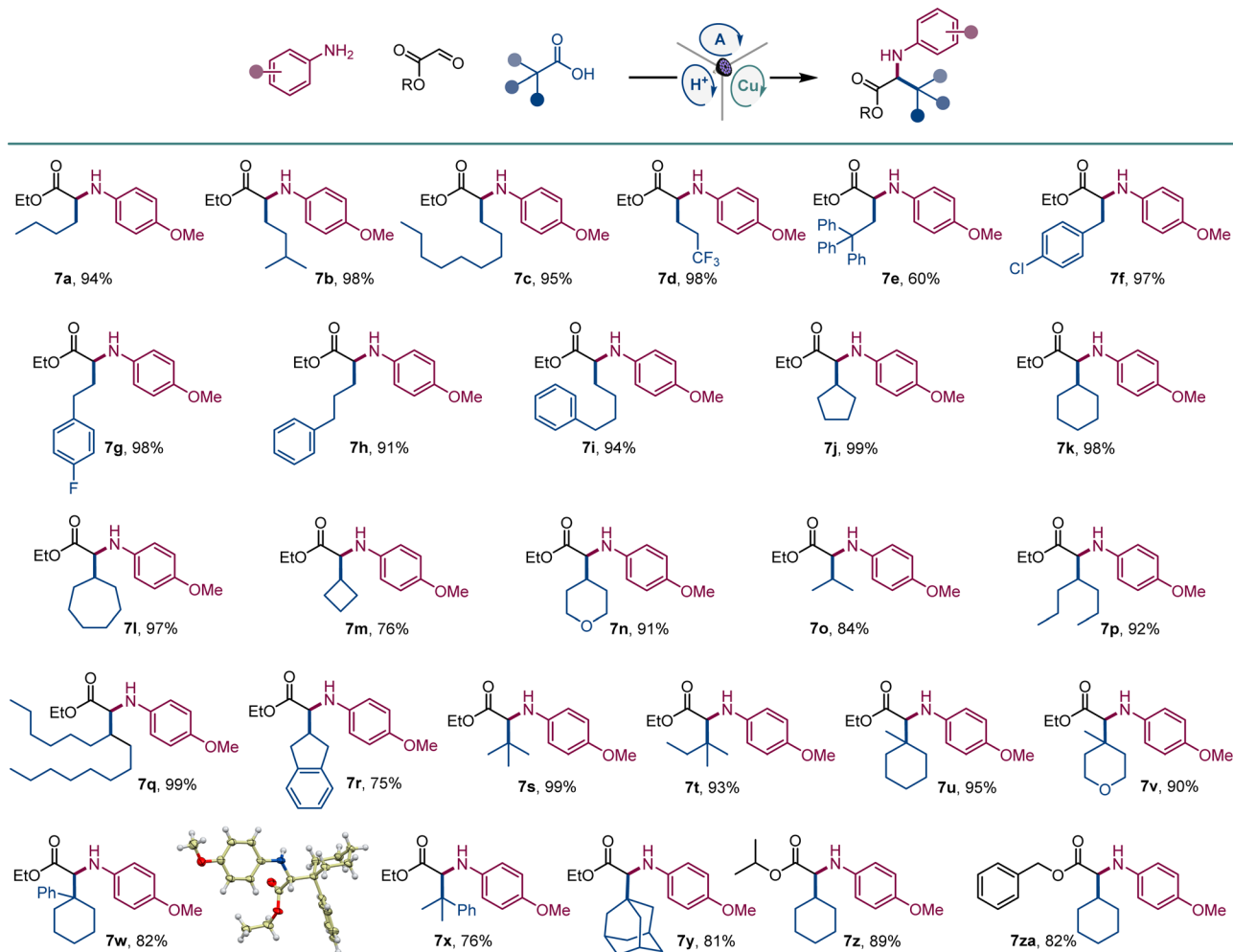


Scheme 3 Scope of carboxylic acids in the direct decarboxylative tricomponent amine construction. Reaction conditions: see Scheme 1.

excellent yields. Likewise, an array of cyclic and acyclic carboxylic acids provided facile segue to amino acid derivatives **7j–7r** featuring diverse secondary alkyl side chains. Notably, the reaction can also be used to access sterically hindered amino acids bearing bulky acyclic and cyclic tertiary alkyl groups (**7s–7y**). The reaction can also be conducted with isopropyl and benzyl glyoxylate, affording corresponding derivatives **7z** and **7za** in high yields.

We also examined the scope of the decarboxylative tricomponent amine construction in the more structurally complex settings of active pharmaceutical ingredients (API) and natural products (Scheme 5). Amines derived from the lipid regulator gemfibrozil (**8a**, **8b**), as well as nonsteroidal anti-inflammatory drugs isoxepac (**8c**) and indomethacin (**8d**) were readily derived from the corresponding coupling partners. Similarly, chenodeoxycholic acid afforded amino acid derivative





Scheme 4 Direct decarboxylative tricomponent construction of α -amino acids. Reaction conditions: see Scheme 1.



Scheme 5 Scope of API and natural product derivatives in the direct decarboxylative tricomponent amine construction. Reaction conditions: see Scheme 1 ^a1 : 1 dr. ^b2 : 1 dr.



8e. Aspartic and glutamic were efficiently converted to orthogonally protected γ -aminoglutamic (**8f**) and δ -aminoglutamic (**8g**) acid derivatives.²¹ Amino acid product **8h** featuring a carbohydrate-derived side chain was similarly easily constructed.

Mechanistic and computational studies were carried out to gain insight into the roles of the catalysts in enabling the tri-component amine construction (Fig. 3). Addition of TEMPO resulted in suppression of the reaction and formation of the corresponding product of cross-termination of TEMPO with the alkyl radical intermediate (**8**, Fig. 3A), pointing to the radical decarboxylative pathway, in line with the reactivity previously observed in other acridine-catalyzed reactions.^{11,16,17}

Kinetic studies indicated that the Brønsted acid catalyst significantly accelerates the imine formation, while no catalytic effect was observed with the copper(I) catalyst and stoichiometric carboxylic acid (Fig. 3B), suggesting that the Brønsted acid facilitates the imine formation in the tri-component process in addition to other potential downstream roles, while the acridine and copper catalysts enable the radical reaction with the imine intermediate.

Computational studies indicated that the alkyl radical addition to imine **9** is kinetically facile and exergonic. The

resulting aminyl radical **10** is further intercepted by the copper catalyst, producing formal copper(II) intermediate **11**. Spin density analysis pointed to the noninnocence of the amido ligand and indicated that the aminyl residue retained most of the radical character after binding to copper. This conclusion is supported by effective oxidation state (EOS) analysis, suggesting that intermediate **11** is best described as a copper(I)-aminyl radical coordination complex. This assignment is in line with previous studies of formal high oxidation state complexes of copper.²²

Subsequent proton-coupled electron transfer with the carboxylic acid produces copper(II) carboxylate **12** whose oxidation state assignment was confirmed by EOS analysis. The ensuing exergonic and barrierless single electron transfer (SET) between copper complex **12** and acridinyl radical **HA** affords copper(I) carboxylate **13** and acridinium cation **HA**⁺ that further regenerate acridine catalyst **A** and the copper catalyst by an exergonic proton transfer.

Interestingly, addition of sulfonic acid also results in an acceleration of the radical addition to imine **9** via a thermodynamically favorable formation of iminium intermediate **14**. The subsequent radical addition proceeds over a lower barrier than for the Brønsted acid-free pathway ($\Delta G^\ddagger = 5.6$ kcal mol⁻¹ for



Fig. 3 (A) Mechanistic studies of the tri-component amine construction. (B) Kinetic profile of imine **9** formation. —●— with TsOH (8 mol%); —■— with acid **3** (1 equiv.); —♦— with Cu(MeCN)₄BF₄ (8 mol%); —▲— uncatalyzed reaction. (C) Computational studies of the radical amine formation, ΔG , kcal mol⁻¹, and the spin density isosurface (isoval = 0.05) for intermediate **11**. R = cyclohexyl, L = MeCN.





Fig. 4 Computational studies of the radical addition to imine **9**. (A) Distortion/interaction activation strain model analysis of **TS1**, **TS2**, and **TS3**, kcal mol⁻¹. (B) Energy decomposition analysis for **TS1** and **TS2**, $\Delta\Delta E_i^{\ddagger} = \Delta E_{\text{TS2}}^{\ddagger} - \Delta E_{\text{TS1}}^{\ddagger}$, kcal mol⁻¹. (C) Complementary occupied-virtual pair (COVP) analysis of **TS2**. The donor orbitals are represented with an opaque surface while acceptor orbitals are represented with a transparent surface. (D) Independent gradient model (IGM) analysis of **TS2**.

TS2 vs. 13.3 kcal mol⁻¹ for **TS1**). Aminium radical cation **10-H** can then be intercepted by the copper catalyst and converted to the amine product by a similar sequence of steps as for aminyl radical **10**. By contrast, the radical addition was less kinetically favorable when the Brønsted acid was replaced by the copper(i) catalyst because of the thermodynamically unfavorable formation of copper-bound imine intermediate **15** that could not be compensated by the reduced barrier to radical addition to complex **15**. Distortion–interaction activated strain model (ASM) analysis²³ indicates that both **TS2** and **TS3** benefit from the substantially stronger interfragment interaction that counterbalances the significantly increased distortion in the case of **TS2** (Fig. 4A). Furthermore, energy decomposition analysis based on absolutely localized molecular orbitals (ALMO-EDA)²⁴ points to the key role of reduced Pauli (steric) repulsion in **TS2** as a consequence of the protonation of the nitrogen atom (Fig. 4B). This observation is congruent with prior studies that pointed to the primary role of reduced Pauli repulsion in the Brønsted acid catalyst-induced acceleration of other reactions.²⁵ Additionally, higher charge transfer, describing interfragment orbital interactions also contributed to the stabilization of **TS2**. Complementary occupied-virtual pair (COVP) analysis of **TS2** points to the radical α -SOMO \rightarrow imine π^* pair as the primary contributor to the charge transfer with the imine $\pi \rightarrow$ radical β -SOMO interaction playing a smaller role (Fig. 4C). Although dispersion was reduced in **TS2**, it contributed to the

interfragment interactions as demonstrated by independent gradient model (IGM) analysis that points to stabilizing interfragment interactions, *e.g.*, a C–H– π interaction between the alkyl radical and the imine fragment. Taken together, these results indicate that the Brønsted acid catalyst may contribute to both in the imine formation and the radical addition phases of the tricomponent amine construction, while the copper catalyst serves as a linchpin between the acridine-catalyzed decarboxylation and the radical amine formation phases by facilitating proton and electron transfer.

Conclusions

In conclusion, we have developed a decarboxylative tricomponent construction of α -branched amines directly from carboxylic acids, aldehydes, and aromatic amines that is enabled by acridine photocatalysis acting in concert with copper and Brønsted acid catalytic cycles. The transformation enables modular access to amines directly from the broad chemical space of carboxylic acids and obviates stepwise preassembly of imines, ketones, and activated carboxylic acid derivatives with a homogeneous photocatalytic system. The reaction provides a streamlined segue to a wide range of α -branched amines bearing α -aromatic substituent, as well as nonproteinogenic α -amino acid derivatives. The scope and functional group tolerance of the tricomponent decarboxylative amine construction



were demonstrated with a range of functionalized aldehydes, aromatic amines, and carboxylic acids, including the structurally complex settings of active pharmaceutical ingredients and natural products. Mechanistic studies revealed the roles of the three intertwined catalytic cycles in enabling the modular amine synthesis and provided a blueprint for further development of direct decarboxylative multicomponent reactions. Unlike homogeneous photocatalytic systems that are based on non-directional single electron transfer that can lead to unselective oxidation of easily oxidizable reagents and products, the triple catalytic system relies on the directional PCET effected by acridine in concert with the supporting copper- and Brønsted acid catalytic cycles, enabling a previously inaccessible homogeneous photocatalytic process.

Data availability

All experimental procedures, characterization data, NMR spectra for all new compounds, and details of the computational studies can be found in the ESI.†

Author contributions

XS, HTD, AP, AD, WTT, and SKD carried out the experiments, and RT, WBH, and SOF performed the computational studies. HDA performed X-ray crystallography studies. OVL directed the project, wrote the manuscript, and co-wrote the ESI.† XS, HTD, AP, AD, SKD, and RT co-wrote the ESI† and contributed to writing the manuscript.

Conflicts of interest

There are no conflicts to declare.

Acknowledgements

Financial support by NSF (CHE-2102646) is gratefully acknowledged. The UTSA NMR, X-ray crystallography, and mass spectrometry facilities were supported by NSF (CHE-1625963, CHE-1920057, CHE-2117691). The authors acknowledge the Texas Advanced Computing Center (TACC) and Advanced Cyberinfrastructure Coordination Ecosystem: Services & Support (ACCESS) for providing computational resources.

Notes and references

- (a) K. L. Skubi, T. R. Blum and T. P. Yoon, *Chem. Rev.*, 2016, **116**, 10035–10074; (b) A. Hossain, A. Bhattacharyya and O. Reiser, *Science*, 2019, **364**, 450; (c) W.-M. Cheng and R. Shang, *ACS Catal.*, 2020, **10**, 9170–9196; (d) A. Y. Chan, I. B. Perry, N. B. Bissonnette, B. F. Buksh, G. A. Edwards, L. I. Frye, O. L. Garry, M. N. Lavagnino, B. X. Li, Y. Liang, E. Mao, A. Millet, J. V. Oakley, N. L. Reed, H. A. Sakai, C. P. Seath and D. W. C. MacMillan, *Chem. Rev.*, 2022, **122**, 1485–1542; (e) K. P. S. Cheung, S. Sarkar and V. Gevorgyan, *Chem. Rev.*, 2022, **122**, 1543–1625.
- (a) E. J. Corey and X.-M. Cheng, *The Logic of Chemical Synthesis*, Wiley, New York, 1995; (b) A. K. Yudin, *Catalyzed Carbon-Heteroatom Bond-Formation*, Wiley-VCH, Weinheim, 2010; (c) S. A. Green, S. W. M. Crossley, J. L. M. Matos, S. Vásquez-Céspedes, S. L. Shevick and R. A. Shenvi, *Acc. Chem. Res.*, 2018, **51**, 2628–2640.
- (a) G. A. Patani and E. J. LaVoie, *Chem. Rev.*, 1996, **96**, 3147–3176; (b) M. Waser, *Asymmetric Organocatalysis in Natural Product Syntheses*, Springer, Vienna, 2012; (c) K. M. Engle and J.-Q. Yu, *J. Org. Chem.*, 2013, **78**, 8927–8955; (d) E. Vitaku, D. T. Smith and J. T. Njardarson, *J. Med. Chem.*, 2014, **57**, 10257–10274; (e) N. Brown, *Mol. Inf.*, 2014, **33**, 458–462.
- Y. Ding, J. P. Ting, J. Liu, S. Al-Azzam, P. Pandya and S. Afshar, *Amino Acids*, 2020, **52**, 1207–1226.
- (a) A. Ray Choudhury and S. Mukherjee, *Chem. Sci.*, 2016, **7**, 6940–6945; (b) H. Park, P. Verma, K. Hong and J.-Q. Yu, *Nat. Chem.*, 2018, **10**, 755–762; (c) Z. Liu, L. J. Oxtoby, M. Liu, Z.-Q. Li, V. T. Tran, Y. Gao and K. M. Engle, *J. Am. Chem. Soc.*, 2021, **143**, 8962–8969.
- (a) S. Patai, *The Chemistry of functional groups, Supplement F2: The chemistry of amino, nitroso, nitro and related group Part 1, 2*, John Wiley & Sons Ltd, Munich, Germany, 1996; (b) A. Ricci, *Methodologies in Amine Synthesis: Challenges and Applications*, Wiley-VCH, Weinheim, Germany, 2021; (c) M. Rivas, V. Palchykov, X. Jia and V. Gevorgyan, *Nat. Rev. Chem.*, 2022, **6**, 544–561.
- (a) J. Yi, S. O. Badir, R. Alam and G. A. Molander, *Org. Lett.*, 2019, **21**, 4853–4858; (b) R. Kumar, N. J. Flodén, W. G. Whitehurst and M. J. Gaunt, *Nature*, 2020, **581**, 415–420; (c) J. H. Blackwell, R. Kumar and M. J. Gaunt, *J. Am. Chem. Soc.*, 2021, **143**, 1598–1609; (d) P. J. Deneny, R. Kumar and M. J. Gaunt, *Chem. Sci.*, 2021, **12**, 12812–12818; (e) X.-K. Qi, L. Guo, L.-J. Yao, H. Gao, C. Yang and W. Xia, *Org. Lett.*, 2021, **23**, 4473–4477; (f) X. Yu, C. G. Daniliuc, F. A. Alasmary and A. Studer, *Angew. Chem., Int. Ed.*, 2021, **60**, 23335–23341; (g) Z. Yao, J. Yang, Z. Luo, H. Wang, X. Zhang, J. Ye, L. Xu and Q. Shi, *Green Chem.*, 2022, **24**, 7968–7973; (h) Q. Li, H. Sun, F. Yan, Y. Zhao, Y. Zhang, C. Zhou, M.-y. Han, H. Li and X. Sui, *Green Chem.*, 2023, **25**, 6226–6230; (i) J. M. Phelps, R. Kumar, J. D. Robinson, J. C. K. Chu, N. J. Flodén, S. Beaton and M. J. Gaunt, *J. Am. Chem. Soc.*, 2024, **146**, 9045–9062.
- T. J. Böttcher, *J. Chem. Inf. Model.*, 2016, **56**, 462–470.
- W. Wei, S. Cherukupalli, L. Jing, X. Liu and P. Zhan, *Drug Discovery Today*, 2020, **25**, 1839–1845.
- W. H. B. Sauer and M. K. Schwarz, *J. Chem. Inf. Model.*, 2003, **43**, 987–1003.
- (a) V. D. Nguyen, G. C. Haug, S. G. Greco, R. Trevino, G. B. Karki, H. D. Arman and O. V. Larionov, *Angew. Chem., Int. Ed.*, 2022, e202210525; (b) H. T. Dang, V. D. Nguyen, G. C. Haug, H. D. Arman and O. V. Larionov, *JACS Au*, 2023, **3**, 813–822.
- (a) J. Guo, Q.-L. Wu, Y. Xie, J. Weng and G. Lu, *J. Org. Chem.*, 2018, **83**, 12559–12567; (b) J. Jia, Q. Lefebvre and M. Rueping, *Org. Chem. Front.*, 2020, **7**, 602–608; (c) A. Shatskiy, A. Axelsson, E. V. Stepanova, J.-Q. Liu, A. Z. Temerdashev,



- B. P. Kore, B. Blomkvist, J. M. Gardner, P. Dinér and M. D. Kärkäs, *Chem. Sci.*, 2021, **12**, 5430–5437; (d) J. Kim, J. K. Lee, B. Moon and A. Lee, *Org. Lett.*, 2022, **24**, 8870–8874; (e) Z. Zhou, Z. S. Sales, D. J. Pippel, M. Qian and C. L. Martin, *J. Org. Chem.*, 2022, **87**, 14948–14952; (f) S. Kim, B. Park, G. S. Lee and S. H. Hong, *J. Org. Chem.*, 2023, **88**, 6532–6537.
- 13 M. Xu, Y. Hua, X. Fu and J. Liu, *Chem. - Eur. J.*, 2022, **28**, e202104394.
- 14 For other recent approaches to α -amino acids, see: (a) I. Eder, V. Haider, P. Zebrowski and M. Waser, *Eur. J. Org. Chem.*, 2021, **2021**, 202–219; (b) Y. Li, J. Yang, X. Geng, P. Tao, Y. Shen, Z. Su and K. Zheng, *Angew. Chem., Int. Ed.*, 2022, **61**, e202210755.
- 15 For recent direct decarboxylative functionalizations, see: (a) Z. Zuo and D. W. C. MacMillan, *J. Am. Chem. Soc.*, 2014, **136**, 5257–5260; (b) J. D. Griffin, M. A. Zeller and D. A. Nicewicz, *J. Am. Chem. Soc.*, 2015, **137**, 11340–11348; (c) J. A. Kautzky, T. Wang, R. W. Evans and D. W. C. MacMillan, *J. Am. Chem. Soc.*, 2018, **140**, 6522–6526; (d) N. A. Till, R. T. Smith and D. W. C. MacMillan, *J. Am. Chem. Soc.*, 2018, **140**, 5701–5705; (e) K. C. Cartwright, S. B. Lang and J. A. Tunge, *J. Org. Chem.*, 2019, **84**, 2933–2940; (f) T. M. Faraggi, W. Li and D. W. C. MacMillan, *Isr. J. Chem.*, 2020, **60**, 410–415; (g) D. Kong, M. Munch, Q. Qiqige, C. J. C. Cooze, B. H. Rotstein and R. J. Lundgren, *J. Am. Chem. Soc.*, 2021, **143**, 2200–2206; (h) D. M. Kitcatt, S. Nicolle and A.-L. Lee, *Chem. Soc. Rev.*, 2022, **51**, 1415–1453; (i) S. Wang, T. Li, C. Gu, J. Han, C.-G. Zhao, C. Zhu, H. Tan and J. Xie, *Nat. Commun.*, 2022, **13**, 2432; (j) S.-C. Kao, K.-J. Bian, X.-W. Chen, Y. Chen, A. A. Martí and J. G. West, *Chem Catal.*, 2023, **3**, 100603; (k) G. A. Lutovsky, S. N. Gockel, M. W. Bundesmann, S. W. Bagley and T. P. Yoon, *Chem*, 2023, **9**, 1610–1621.
- 16 (a) V. T. Nguyen, V. D. Nguyen, G. C. Haug, H. T. Dang, S. Jin, Z. Li, C. Flores-Hansen, B. Benavides, H. D. Arman and O. V. Larionov, *ACS Catal.*, 2019, **9**, 9485–9498; (b) H. T. Dang, G. C. Haug, V. T. Nguyen, N. T. H. Vuong, H. D. Arman and O. V. Larionov, *ACS Catal.*, 2020, **10**, 11448–11457; (c) V. T. Nguyen, V. D. Nguyen, G. C. Haug, N. T. H. Vuong, H. T. Dang, H. D. Arman and O. V. Larionov, *Angew. Chem., Int. Ed.*, 2020, **59**, 7921–7927; (d) V. T. Nguyen, G. C. Haug, V. D. Nguyen, N. T. H. Vuong, H. D. Arman and O. V. Larionov, *Chem. Sci.*, 2021, **12**, 6429–6436; (e) V. T. Nguyen, G. C. Haug, V. D. Nguyen, N. T. H. Vuong, G. B. Karki, H. D. Arman and O. V. Larionov, *Chem. Sci.*, 2022, **13**, 4170–4179; (f) V. D. Nguyen, R. Trevino, S. G. Greco, H. D. Arman and O. V. Larionov, *ACS Catal.*, 2022, **12**, 8729–8739; (g) H. T. Dang, A. Porey, S. Nand, R. Trevino, P. Manning-Lorino, W. B. Hughes, S. O. Fremin, W. T. Thompson, S. K. Dhakal, H. D. Arman and O. V. Larionov, *Chem. Sci.*, 2023, **14**, 13384–13991; (h) A. Porey, S. O. Fremin, S. Nand, R. Trevino, W. B. Hughes, S. K. Dhakal, V. D. Nguyen, S. G. Greco, H. D. Arman and O. V. Larionov, *ACS Catal.*, 2024, **14**, 6973–6980.
- 17 (a) M. O. Zubkov, M. D. Kosobokov, V. V. Levin, V. A. Kokorekin, A. A. Korlyukov, J. Hu and A. D. Dilman, *Chem. Sci.*, 2020, **11**, 737–741; (b) I. A. Dmitriev, V. V. Levin and A. D. Dilman, *Org. Lett.*, 2021, **23**, 8973–8977; (c) M. O. Zubkov, M. D. Kosobokov, V. V. Levin and A. D. Dilman, *Org. Lett.*, 2022, **24**, 2354–2358; (d) K. A. Zhilyaev, D. L. Lipilin, M. D. Kosobokov, A. I. Samigullina and A. D. Dilman, *Adv. Synth. Catal.*, 2022, **364**, 3295–3301; (e) A. Adili, A. B. Korpusik, D. Seidel and B. S. Sumerlin, *Angew. Chem., Int. Ed.*, 2022, **61**, e202209085; (f) K. A. Zhilyaev, D. L. Lipilin, M. D. Kosobokov, A. I. Samigullina and A. D. Dilman, *Adv. Synth. Catal.*, 2022, **364**, 3295–3301; (g) J. A. Andrews, J. Kalepu, C. F. Palmer, D. L. Poole, K. E. Christensen and M. C. Willis, *J. Am. Chem. Soc.*, 2023, **145**, 21623–21629; (h) J. G. L. de Araujo, M. d. S. B. da Silva, J. C. C. V. Bento, A. M. de Azevêdo, A. M. de M. Araújo, A. S. D. dos Anjos, C. A. Martínez-Huitle, E. V. dos Santos, A. D. Gondim and L. N. Cavalcanti, *Chem. - Eur. J.*, 2023, **29**, e202302330; (i) D. L. Lipilin, M. O. Zubkov, M. D. Kosobokov and A. D. Dilman, *Chem. Sci.*, 2024, **15**, 644–650.
- 18 A related decarboxylative construction of amines from *in situ* generated azometines has also been recently reported: Z. M. Rubanov, V. V. Levin and A. D. Dilman, *Org. Lett.*, 2024, **26**, 3174–3178.
- 19 J. C. Suatoni, R. E. Snyder and R. O. Clark, *Anal. Chem.*, 2002, **33**, 1894–1897.
- 20 (a) F. Palacios, J. Vicario and D. Aparicio, *J. Org. Chem.*, 2006, **71**, 7690–7696; (b) U. Bhakta, P. V. Kattamuri, J. H. Siitonen, L. B. Alemany and L. Kürti, *Org. Lett.*, 2019, **21**, 9208–9211.
- 21 A. Chikugo, Y. Irie, C. Tsukano, A. Uchino, T. Maki, T. Kume, T. Kawase, K. Hirose, Y. Kageyama, I. Tooyama and K. Irie, *ACS Chem. Neurosci.*, 2022, **13**, 2913–2923.
- 22 I. M. DiMucci, J. T. Lukens, S. Chatterjee, K. M. Carsch, C. J. Titus, S. J. Lee, D. Nordlund, T. A. Betley, S. N. MacMillan and K. M. Lancaster, *J. Am. Chem. Soc.*, 2019, **141**, 18508–18520.
- 23 F. M. Bickelhaupt and K. N. Houk, *Angew. Chem., Int. Ed.*, 2017, **56**, 10070–10086.
- 24 R. Z. Khaliullin, E. A. Cobar, R. C. Lochan, A. T. Bell and M. Head-Gordon, *J. Phys. Chem.*, 2007, **111**, 8753–8765.
- 25 S. Yu, F. M. Bickelhaupt and T. A. Hamlin, *ChemistryOpen*, 2021, **10**, 784–789.

